Published in final edited form as:
Sci Signal. ; 3(114): ra22. doi:10.1126/scisignal.2000818.

Gain-of-function enhancement of $InsP_3$ receptor modal gating by familial Alzheimer's disease-linked presenilin mutants in human cells and mouse neurons

King-Ho Cheung[1], **Lijuan Mei**[1], **Don-On Daniel Mak**[1], **Ikuo Hayashi**[2], **Takeshi Iwatsubo**[2], **David E. Kang**[3], and **J. Kevin Foskett**[1,4,*]

[1]Department of Physiology, University of Pennsylvania, Philadelphia, PA 19104 USA

[2]Department of Neuropathology and Neuroscience, University of Tokyo, Tokyo 113-0033, Japan

[3]Department of Neurosciences, University of California, San Diego, La Jolla, CA 92093 USA

[4]Department of Cell and Developmental Biology, University of Pennsylvania, Philadelphia, PA 19104 USA

Abstract

Familial Alzheimer's disease (FAD) is caused by mutations in amyloid precursor protein or presenilins (PS1, PS2). Many FAD-linked PS mutations affect intracellular calcium (Ca^{2+}) homeostasis by mechanisms proximal to and independent of amyloid production, although the molecular details are controversial. Here, we demonstrate that several FAD-causing PS mutants enhance gating of the inositol trisphosphate receptor ($InsP_3R$) Ca^{2+} release channel by a gain-of-function effect that mirrors the genetics of FAD and is independent of secretase activity. In contrast, wild type PS or PS mutants that cause frontotemporal dementia have no such effect. FAD PS alter $InsP_3R$ channel gating by modal switching. Recordings of endogenous $InsP_3R$ in lymphoblasts derived from individuals with FAD or cortical neurons of asymptomatic PS1-AD mice revealed they have higher occupancy in a high open probability burst mode compared to that of $InsP_3R$ in cells with wild-type PS, resulting in enhanced Ca^{2+} signaling. These results indicate that exaggerated Ca^{2+} signaling through $InsP_3R$-PS interaction is a disease-specific and robust proximal mechanism in FAD.

INTRODUCTION

Alzheimer's disease (AD) is a common form of dementia that involves slowly developing and ultimately fatal neurodegeneration. Most AD is sporadic and idiopathic and develops at ages over 60, but about 5% is inherited in an autosomal dominant manner due to mutations in amyloid precursor protein (APP) or presenilins (PS1, PS2) (1). Although familial Alzheimer's disease (FAD) develops at ages as early as the late 30s, both familial and sporadic AD share hallmark features that include accumulation of β amyloid (Aβ) in extracellular plaques, intracellular neurofibrillary tangles comprised largely of hyper-phosphorylated tau, and cell atrophy and death in various brain regions (2–4). The consistent phenotypes suggest that both types of AD may share pathogenic origins. Nevertheless, the mechanisms by which these mutant proteins exert such devastating effects, and their roles and relationships in the two forms of AD, are still not clear. Insights into the molecular mechanisms and cellular functions of

*Correspondence should be addressed to: J. Kevin Foskett, PhD (foskett@mail.med.upenn.edu), Department of Physiology, B39 Anatomy-Chemistry Bldg/6085, University of Pennsylvania, Philadelphia, PA 19104-6085.

mutant proteins in FAD are likely to provide important clues into the etiology of AD pathogenesis and the identification of targets for therapeutic interventions.

Presenilins are transmembrane proteins that are synthesized on the endoplasmic reticulum (ER) and localized there (5). Together with nicastrin, APH-1 (anterior pharynx-defective 1), and PEN-2 (presenilin enhancer 2), PS forms a protein complex that is transported to the cell surface and to endosomes, where it functions as a γ-secretase that cleaves several type 1 transmembrane proteins, including APP (6,7). γ-secretase cleavage of APP releases Aβ peptides, a major component of amyloid plaques in the brains of AD patients. Mutant PS are believed to affect APP processing by either enhancing the total production of Aβ or the relative proportion of the more amyloidogenic Aβ-42 form (8). In the amyloid hypothesis of AD, accumulation of amyloidogenic Aβ aggregates or oligomers is a proximal feature that causes neural toxicity leading to brain pathology (9,10). However, FAD mutations in PS cause loss of secretase function, in contrast with the dominant gain-of-function indicated by the genetics of the disease (11). In addition to disrupting APP processing, many FAD-linked PS mutations affect intracellular calcium (Ca^{2+}) homeostasis (12,13). Although extracellular Aβ influences intracellular Ca^{2+} homeostasis in vitro (14,15) and in vivo (16,17), FAD-mutant PS also influences intracellular Ca^{2+} signaling by proximal, Aβ-independent mechanisms. Such Ca^{2+} signaling disruptions have manifested as attenuated capacitive Ca^{2+} entry (18–20), but most commonly as exaggerated Ca^{2+} liberation from the ER (18,21–24), the major intracellular Ca^{2+} storage organelle. The molecular mechanisms underlying exaggerated ER Ca^{2+} release have been ascribed to enhanced loading of the ER lumen (23) due either to enhanced SERCA (sarco-endoplasmic reticulum Ca^{2+}-ATPase) pump activity (25) or to disruption of a putative Ca^{2+} channel function of wild-type PS (26,27). Alternately, exaggerated Ca^{2+} release has been accounted for by enhanced Ca^{2+} liberation from normal stores through inositol trisphosphate receptor ($InsP_3R$) (21,23) or ryanodine receptor (RyR) (22,28,29) Ca^{2+} release channels, both in vivo (22,24,28,29) and in vitro (30–33), either as a consequence of enhanced channel abundance (28,34–36) or, in the case of the $InsP_3R$, enhanced activity in response to its ligand $InsP_3$ (32,37). Notably, enhanced agonist-induced $InsP_3R$-mediated Ca^{2+} signals have been used diagnostically to identify individuals with FAD (31,32). Biochemical interaction of the $InsP_3R$ with both wild-type (WT) and FAD-mutant PS1 and PS2 has been demonstrated (37). Single channel recordings of Sf9 insect cell $InsP_3R$ demonstrated that recombinant FAD-mutant PS1 and a FAD mutant-PS2 could enhance $InsP_3R$ Ca^{2+} release channel gating (37). These single channel studies were performed in the absence of Aβ or cellular pathology, suggesting that modulation of $InsP_3R$ gating is a fundamental mechanism that contributes to exaggerated Ca^{2+} signaling in FAD PS-expressing cells.

It is not known whether the effects of FAD PS on $InsP_3R$ gating represent a gain or loss of function. Moreover, although many (>100) PS mutations (especially in PS1) that cause FAD have been identified (38), only two FAD-mutant PS have been examined for their effects on $InsP_3R$ channel gating (37). In addition, some PS1 mutations result in frontotemporal dementia (FTD), a neurological disorder lacking Aβ accumulation (39,40). If FAD PS-mediated alteration of $InsP_3R$-mediated Ca^{2+} signaling is proximal in AD pathogenesis, then other FAD-mutant PS might be expected to have similar enhancing effects on $InsP_3R$ channel gating, whereas those associated with FTD might not. Previous studies of the effects of mutant PS on $InsP_3R$ investigated endogenous insect (Sf9 ovarian cells) and chicken (DT40 B lymphocytes) $InsP_3Rs$ (37), whereas AD, in which the pathological consequences are primarily in brain neurons, affects humans. Consequently, the relevance of these data in appropriate cell types with endogenous amounts of PS and $InsP_3R$ are unclear. Here, we studied $InsP_3R$ channel kinetics under the influence of several FAD- and FTD-mutant PS in four different systems, including transgenic AD mouse neurons, B-lymphoblasts derived from human FAD patient cells, and fibroblasts from PS 1 and 2 double knock-out cells. All FAD-linked PS mutations enhanced $InsP_3R$ single channel gating, leading to exaggerated intracellular Ca^{2+} signaling,

whereas FTD-associated PS1 mutations did not affect $InsP_3R$ channel kinetics. Furthermore, the effects of FAD PS mutants were gain-of-function effects, consistent with the genetics of FAD. In contrast, the secretase activity of PS was not required. The results indicate that exaggerated Ca^{2+} signaling through $InsP_3R$-PS interaction is a disease-specific and robust proximal mechanism in FAD.

RESULTS

Multiple FAD PS mutations modulate $InsP_3R$ channel gating by mode switching

To determine whether enhanced $InsP_3R$ channel activity is a phenotype conserved in FAD PS-expressing cells, we recorded single $InsP_3R$ channel activities in the presence of one of eight different PS mutants (PS1-L113P (leucine at residue 113 substituted with proline), -M146L, -L166P, -G183V, -D257A, -G384A, -D385A and PS2-N141I). We performed single-channel patch-clamp electrophysiology of the outer membrane of isolated Sf9 cell nuclei (41) 48 hr after infecting cells with recombinant baculovirus (Fig. S1). Because enhancement of $InsP_3R$ activity is more apparent at sub-saturating $InsP_3$ concentrations (37), we used 100 nM $InsP_3$ and 1 μM Ca^{2+} to sub-optimally activate channel gating. We consistently detected $InsP_3R$ channels with open probability (P_o) of 0.27 ± 0.04 in membrane patches from control EVER1- (an irrelevant ER transmembrane protein) infected nuclei (Fig. 1A and B). $InsP_3R$ channels recorded in membrane patches from PS1-WT- or PS2-WT-infected cells had P_o similar to those from EVER1-infected control cells (P_o = 0.32 ± 0.04 and 0.25 ± 0.03, respectively; p >0.05; Fig. 1A and B). In contrast, $InsP_3R$ channel P_o was significantly enhanced by 250% in nuclei from cells infected with mutant PS1-M146L (P_o = 0.81 ± 0.02; Fig. 1A and B) to a degree similar to that achieved with saturating ligand concentrations (37). Increased P_o resulted from a marked reduction of channel mean closed-time (τ_c; Fig. 1C). FAD-mutant PS2 (N141I) also markedly enhanced $InsP_3R$ channel activity (Fig. 1A and B), with P_o increased by 200% (0.66 ± 0.05; Fig. 1B), also mainly due to a significant reduction of τ_c (Fig. 1C). Similar results were obtained for two other FAD-causing PS1 mutants: $InsP_3R$ channel P_o was increased 200% with PS1-L166P (P_o = 0.63 ± 0.08) or PS1-G384A (P_o = 0.61 ± 0.05; Fig. 1A and B). Thus, all four FAD PS mutants examined had similar effects on $InsP_3R$ channel activity. The γ-secretase-dead mutants PS1-D257A and PS1-D385A, which have mutations in intra-membrane sites involved in PS1 catalytic activity, also significantly enhanced $InsP_3R$ channel activity, although to a lesser extent than the FAD mutants (P_o = 0.50 ± 0.05 and 0.46 ± 0.08, respectively; Fig. 1A and B). Thus, the secretase activity of PS is not required for its effects on $InsP_3R$ gating. P_o of channels recorded from cells infected with FTD-associated mutant PS1-L113P and PS1-G183V were 0.28 ± 0.04 and 0.29 ± 0.04, respectively, not different from controls (Fig. 1A and B). Thus, several FAD-mutant PS have similar effects on $InsP_3R$ gating, and these effects are not recapitulated in PS mutants associated with a different neurological disease.

To gain deeper insight into the mechanisms of $InsP_3R$ channel activation by FAD-mutant PS, we employed modal gating analysis. Previous studies demonstrated that ligand ($InsP_3$, Ca^{2+}) regulation of $InsP_3R$ gating is largely mediated by altering the propensity of the channel to gate in particular modes (42). Strongly activated channels gate in a high-P_o H mode characterized by long bursting activities; an intermediate-P_o I mode is characterized by fast channel openings and closings; and a low-P_o L mode is characterized by long closed periods containing brief openings (42). In control nuclei isolated from EVER1-infected cells, the L gating mode was dominant, with the channel spending ~60% of its time in this mode and ~25% in the H mode (Fig. 1D). In nuclei from cells infected with either WT or FTD PS, similar modal gating distributions were observed (Fig. 1D). In contrast, the H mode was the dominant gating mode of $InsP_3R$ recorded from all of the FAD-causing mutant PS-expressing cells (Fig. 1D).

Thus, FAD-mutant PS enhance $InsP_3R$ channel gating by mode switching, causing the channel to spend more time in the H mode at the expense primarily of the L mode (Fig. 1D; Fig. S2).

$InsP_3R$ single channel gating and $InsP_3$-mediated Ca^{2+} signals are enhanced in human FAD B cells

Enhancement of $InsP_3R$ channel activity by heterologous expression of mutant PS has been demonstrated in both Sf9 and DT40 cells [(37) and this study], systems that employ PS over-expressed in non-human cells. To determine the effects of endogenous PS in human cells, we studied $InsP_3R$ activity in normal and FAD human B cell lymphoblasts. Currents from endogenous human $InsP_3R$ single channels have never been previously recorded. Thus, we initially characterized endogenous $InsP_3R$ channels from human B lymphoblasts by nuclear membrane patch-clamp electrophysiology. In the absence of $InsP_3$, no channel activity was apparent (n = 18; Fig. 2B), whereas with $InsP_3$ (10 μM) in the pipette solution, we observed heparin-sensitive single channels with brief openings and long closings (n =15; Fig. 2A and B). These channels showed a linear *I/V* relationship with slope conductance ~475 pS (Fig. 2C), typical of mammalian $InsP_3R$ under these ionic conditions (43). $InsP_3R$ currents recorded from human B cells were long-lasting (Fig. 2A), with relatively low P_o (0.18 ± 0.02, n=20; Fig. 2D).

We compared $InsP_3R$ gating in B lymphoblasts derived from three individuals with FAD, harboring PS1-M146L, PS1-A246E, or PS2-N141I (FAD lymphocytes), with that in B-lymphoblasts from two different age-matched individuals without FAD or FAD-associated PS mutations (control lymphoblasts) (Table 1). $InsP_3R$ in control lymphoblasts from the two individuals without FAD had low channel P_o (0.18 ± 0.02 and 0.23 ± 0.03, respectively; Fig. 3A,B) with channel activities characterized by brief openings and relatively long closings (Fig. 3A and C). $InsP_3R$ P_o recorded from lymphoblasts from all three individuals with FAD were increased 200 to 300% when compared with those from control lymphoblasts (PS1-M146L: 0.62 ± 0.05; PS1-A246E: 0.67± 0.06; PS2-N141I: 0.50 ± 0.04; Fig. 3A and B), mainly due to a marked decrease in τ_c (Fig. 3C), with many channels bursting for extended periods (Fig. 3E). In control lymphoblasts, the L and I gating modes dominated channel kinetics, whereas $InsP_3R$ analyzed in FAD lymphoblasts spent 50 to 75% of the time in the high P_o H mode (Fig. 3D and E). Analogous results were obtained with low (100 nM) $InsP_3$. $InsP_3R$ P_o was 0.04 ± 0.01 in control lymphoblasts from an individual without FAD, whereas P_o was 0.22 ± 0.05 in PS1-A246E FAD lymphoblasts (Fig. 3F–G). These observations in human B-lymphoblasts with endogenous PS and $InsP_3R$ are similar to those made in Sf9 and DT40 cells. FAD-linked PS mutations therefore have a robust, common effect to enhance $InsP_3R$ single channel activity in insect, avian, and human cells.

To determine whether these effects observed at the single-channel level are associated with altered $[Ca^{2+}]_i$ signaling, we measured $InsP_3R$-mediated Ca^{2+} signals in B lymphoblasts from the same individuals with FAD that were used for single-channel studies. $InsP_3R$-mediated Ca^{2+} signals were elicited by cross-linking the B cell receptor (BCR) with IgM antibody. At high [IgM] (5μg/ml), 20% of cells responded with similar Ca^{2+} oscillations and spiking in both control and PS1-A246E FAD lymphoblasts (Fig. 4B and D), whereas a further 27% of the FAD lymphoblasts responded with exaggerated high-amplitude transient responses (Fig. 4A, B and C). With low-dose anti-IgM stimulation (50 ng/ml), Ca^{2+} oscillations/spiking were triggered in 19% ± 2% of control cells (Fig. 4E and G). Perfusion with xestospongin B, a membrane-permeable specific $InsP_3R$ inhibitor (44), reversibly inhibited them indicating that they were due to periodic Ca^{2+} release through the $InsP_3R$ (Fig. S3). In FAD lymphoblasts, both the percentage of responding cells and the oscillation and spiking frequency were increased (Fig. 4E, G and H). Perfusion with culture medium containing 10% FBS, which generates ongoing low $InsP_3$ production (45), induced spontaneous Ca^{2+} oscillations/spiking in 25 ± 5% of control lymphoblasts (Fig. 4F and G). In contrast, the percentage of PS1 FAD lymphocytes displaying

spontaneous Ca^{2+} oscillations was increased by 100% and the oscillation and spiking frequency doubled (Fig. 4F, G and H). The percentage of spontaneously oscillating PS2-N141I FAD cells was similar to that in control lymphoblasts, however, the oscillation frequency was increased (Fig. 4F, G and H). These responses are consistent with an enhanced sensitivity and activity of $InsP_3$-mediated Ca^{2+} release in human FAD lymphoblasts, consistent with the enhanced $InsP_3R$ channel activity recorded in these cells.

$InsP_3R$ channel gating is enhanced in FAD mouse cortical neurons

Ca^{2+} signaling disruption has been observed in fibroblast or lymphoblast lines derived from human FAD cells [here and (30,32,46)]. Our results above implicate mutant PS-enhanced $InsP_3R$ channel gating as the underlying mechanism. To determine if this molecular mechanism also operates in brain neurons, we isolated cortical neurons from embryonic day 14 to 16 (E14 to E16) WT C57BL/6 and 3×Tg-AD mice and recorded single $InsP_3R$ channel activities in nuclear envelopes from isolated nuclei. 3xTg-AD mice contain PS1-M146V knocked into the PS1 locus, and exhibit age-dependent amyloid plaques, neurofibrillary tangles, and cognitive decline starting at 3 to 6 months of age (3,47). In nuclei isolated from control C57BL/6 mice, channel currents were not observed in the absence of $InsP_3$ (Fig. 5B). With 10 μM $InsP_3$, and 1 μM Ca^{2+}, heparin-sensitive (Fig. 5B), channels with a linear slope conductance of ~375 pS (Fig. 5C) were recorded (Fig. 5A and B) with gating characterized by short openings (τ_o = 2.25 ± 0.11 ms) and relatively long closures (τ_c = 52.7 ± 12.7 ms) with P_o = 0.06 ± 0.01 (Fig. 5D). P_o was enhanced by 700% (0.43 ± 0.05; Fig. 5B and D) in nuclei isolated from 3xTg-AD mice. Increased P_o was caused by markedly prolonged τ_o (10.22 ± 1.57 ms) together with shortened τ_c (14.61 ± 3.04 ms). The I and L modes dominated channel gating in control C57BL/6 neurons, whereas the H mode was the major gating mode in 3xTg-AD neurons (Fig. 5B,E, and F).

FAD PS enhancement of $InsP_3R$ channel gating is a gain-of-function effect

Our results reveal that FAD-mutant PS consistently enhances $InsP_3R$ channel gating. To explore the mechanisms involved, we recorded endogenous $InsP_3R$ channels in nuclei from embryonic fibroblasts (MEF) derived from PS double-knockout mice (48,49). In the absence of PS, the endogenous MEF $InsP_3R$ P_o was 0.30 ± 0.03 (Fig. 6). Stable expression of human PS1 by retroviral transduction was without effect on $InsP_3R$ P_o (0.27 ± 0.05), whereas FAD mutant PS1-M146L approximately doubled channel gating activity (0.54 ± 0.05), by enhancing H-mode gating (Fig. 6). Similar results were obtained in independently-derived MEF clones (Fig. S4). These results indicate that the effects of FAD-mutant PS on $InsP_3R$ channel involve a gain of function. As shown above in Sf9 cells, this function is independent of PS secretase activity, because the secretase-dead PS1-D257A also enhanced channel activity (Fig. 6).

DISCUSSION

In summary, the above results demonstrate a consistent and robust phenotype associated with the presence of mutant PS linked to FAD. In five different cell systems (four here and DT40 cells previously) from four species, FAD-causing mutant PS resulted in exaggerated responses of $InsP_3R$ Ca^{2+} release channels and exaggerated Ca^{2+} signals in response to agonist stimulation, as well as a small degree of constitutive Ca^{2+} signaling. The FAD-mutant PS phenotype involves gain-of-function effects, consistent with disease genetics, and is independent of the secretase function of PS. Moreover, the FAD-mutant PS phenotype is not observed in cells harboring either wild-type PS or PS mutants associated with a different disease, FTD. The FAD-mutant PS phenotype is manifested independently of any pathology associated with AD, and, in the mouse model, precedes such pathology. Moreover, it is apparent in physiologically-relevant cell types (cells derived from humans with FAD and AD mouse neurons) with all proteins present in endogenous amounts. We propose that exaggerated

Ca^{2+} signaling through an $InsP_3R$-PS interaction is a robust proximal gain-of-function molecular mechanism in FAD.

Our single channel analyses demonstrate that FAD-mutant PS enhances single channel activity of the $InsP_3R$ by affecting modal gating kinetics, the major mechanism by which $InsP_3$ and Ca^{2+} regulate the channel (42). That FAD-mutant PS drives the channel into the H mode may have important physiological implications. The channel open time when it in the L gating mode (~10 ms) is short enough that it may not increase local $[Ca^{2+}]$ sufficiently to recruit additional $InsP_3R$- or RyR-mediated Ca^{2+} release by Ca^{2+}-induced Ca^{2+} release (CICR). In contrast, the much longer activity bursts of the channel in the H mode (>200 ms) will provide a sufficiently large flux of Ca^{2+} to enable a normally local Ca^{2+} signal to be amplified and propagated by CICR (50). Because $InsP_3R$ and RyR are clustered and spatially localized to different regions of cells to provide local $[Ca^{2+}]_i$ signals as a critical element of physiological specificity, mode-shifting by mutant PS-induced FAD may result not only in exaggerated local Ca^{2+} signaling, but also a disruption of spatial specificity by enabling CICR to transmit the signals more globally (42,50). Exaggerated and spatially disrupted Ca^{2+} signaling may in turn impinge on APP processing (16,51–54), calpain activation (16,54), and tau phosphorylation (55,56), linking our findings here to the amyloid hypothesis of AD (Fig. 7).

MATERIALS AND METHODS

Cell Culture

Spodoptera frugiperda cells (Sf9, BD Biosciences) were maintained as described (37,41). Human PS baculovirus constructs (PS1-WT, PS1-L113P, PS1-M146L, PS1-L166P, PS1-G183V, PS1-D257A, PS1-G384A, PS1-D384A, PS2-WT and PS2-N141I) were subcloned into pFastBac1 and baculoviruses were generated using the Bac-to-Bac system (Invitrogen). Expression was confirmed by Western blotting with antibodies directed against PS1 or PS2 (anti-PS1 and anti-PS2, respectively) as described (37). B-lymphoblast lines derived from human FAD patients and normal individuals (Table I; Coriell Institute, Camden, NJ) were maintained at 37°C (95/5% air/CO_2) in RPMI 1640 (Invitrogen) supplemented with 15% fetal bovine serum (Hyclone), 2 mM L-glutamine, 100 units/ml penicillin, and 100 μg/ml streptomycin. $PS^{-/-}$ (genetically deficient in PS1 and PS2), stable human PS1-WT, mutant PS1-M146L and PS1-D257A MEF cells were grown in DMEM supplemented with 10% fetal bovine serum (57,58). To generate stable lines expressing comparable amounts of PS1 proteins, human PS1 cDNAs were introduced into pMX-IRES-EGFP retroviral vector, and PS retroviruses generated using Retro-X system (Clontech) were added to the parental $PS^{-/-}$ MEF cells, and GFP positive cells were sorted by FACS. PS expression was confirmed by Western blot.

Cortical neuron isolation

Primary cortical neurons were prepared from embryonic day 14 to 16 (E14 to E16) 3xTg-AD mice as described (37). Neurons from C57BL/6 mice (Charles River) served as controls. In brief, dams were killed with CO_2, and embryos were removed by cesarean section. Brains from littermates were removed and placed into PBS. After the meninges were removed, cerebral cortices were dissected, minced, and digested with 0.25% trypsin in PBS at 37°C for 20 min. Dissociated cells were washed twice with DMEM supplemented with 10% FBS, triturated with a fire-polished Pasteur pipette and re-suspended in Neurobasal medium supplemented with 1x B27 (Invitrogen). All animal procedures were approved by the University of Pennsylvania Institutional Animal Care and Use Committee (IACUC).

Calcium imaging

Human B-lymphoblasts (Coriell Institute, Camden, NJ) were plated onto a CellTek-(BD Biosciences) coated glass-bottom perfusion chamber mounted on the stage of an inverted microscope (Eclipse TE2000; Nikon, Melville, NY) and incubated with fura-2 AM (2 μM; Invitrogen) for 30 min at room temperature in Hanks' balanced salt solution (HBSS, Sigma, St. Louis, MO) containing 1% BSA. Cells were then continuously perfused with HBSS containing 1.8 mM $CaCl_2$ and 0.8 mM $MgCl_2$ (pH 7.4). Ca^{2+} signals were elicited by cross-linking the B cell receptor (BCR) with 50 ng/ml anti-human IgM antibody (SouthernBiotech, Birmingham, AL). In some experiments, cells were perfused with complete culture medium containing 10% FBS. Fura-2 was alternately excited at 340 and 380 nm, and the emitted fluorescence filtered at 510 nm was collected and recorded (37,45) using a CCD-based imaging system running Ultraview software (PerkinElmer, Waltham, MA). Dye calibration was achieved by applying experimentally determined constants to the standard equation $[Ca^{2+}] = K_d \cdot \beta \cdot (R - R_{min})/(R_{max} - R)$.

Electrophysiology

Preparation of isolated nuclei from cells was performed as described (37,41,45). In brief, cells were washed twice with PBS and suspended in nuclear isolation solution containing (in mM): 150 KCl, 250 sucrose, 1.5 β-mercapoethanol, 10 Tris-HCl, 0.05 phenylmethylsulphonyl fluoride and protease inhibitor cocktail (Complete, Roche Diagnosis, Indianapolis, IN), pH 7.3. Nuclei were isolated using a Dounce glass homogenizer and plated onto a 1-ml glass-bottomed dish containing standard bath solution (in mM): 140 KCl, 10 HEPES, 0.5 BAPTA, and 0.192 $CaCl_2$ (free $[Ca^{2+}]$ = 90 nM). The pipette solution contained (in mM): 140 KCl, 10 HEPES, 0.5 dibromo-BAPTA, and 0.001 free Ca^{2+}, pH 7.3. Free $[Ca^{2+}]$ in solutions was adjusted by Ca^{2+} chelators with appropriate affinities and confirmed by fluorometry as described (41). Data were recorded at room temperature and acquired using an Axopatch 200A amplifier (Axon Instruments), filtered at 1 kHz, and digitized at 5 kHz with an ITC-16 interface (Instrutech) and Pulse software (HEKA Electronik).

Data Analysis

Segment of current records exhibiting current levels for a single $InsP_3R$ channel were idealized using QuB software (University of Buffalo) with SKM algorithm (59,60). Channel gating kinetics and modal gating behaviors were characterized as described (42). In brief, very short closing events (< 10 ms), presumably caused by ligand-independent transitions, were removed by burst analysis (61) after idealization with QuB. Modal gating assignment was then achieved by plotting and examining durations of channel burst (t_b) and burst-terminating gaps (t_g) as described (42). In Sf9 cells, we set T_b =100 ms and T_g = 200 ms for the detection of modal transitions. In both human B-lymphocytes and mouse cortical neurons, we set T_b = 50 ms and T_g = 100 ms for the detection of modal transitions. Data were summarized as the mean ± SEM, and the statistical significance of differences between means was assessed by using unpaired t tests or one-way ANOVA with Dunnett's post hoc comparison test. Differences between means were accepted as statistically significant at the 95% level (p <0.05).

Supplementary Material

Refer to Web version on PubMed Central for supplementary material.

REFERENCES

1. Hutton M, Hardy J. The presenilins and Alzheimer's disease. Hum. Mol. Genet 1997;6:1639–1646. [PubMed: 9300655]
2. Hardy J. A hundred years of Alzheimer's disease research. Neuron 2006;52:3–13. [PubMed: 17015223]

3. LaFerla FM, Oddo S. Alzheimer's disease: Abeta, tau and synaptic dysfunction. Trends. Mol. Med 2005;11:170–176. [PubMed: 15823755]
4. Mattson MP. Pathways towards and away from Alzheimer's disease. Nature 2004;430:631–639. [PubMed: 15295589]
5. Annaert WG, Levesque L, Craessaerts K, Dierinck I, Snellings G, Westaway D, George-Hyslop PS, Cordell B, Fraser P, De Strooper B. Presenilin 1 controls gamma-secretase processing of amyloid precursor protein in pre-golgi compartments of hippocampal neurons. J. Cell. Biol 1999;147:277–294. [PubMed: 10525535]
6. De Strooper B, Saftig P, Craessaerts K, Vanderstichele H, Guhde G, Annaert W, Von Figura K, Van Leuven F. Deficiency of presenilin-1 inhibits the normal cleavage of amyloid precursor protein. Nature. 1998;391:387–390.
7. Li H, Wolfe MS, Selkoe DJ. Toward structural elucidation of the gamma-secretase complex. Structure 2009;17:326–334. [PubMed: 19278647]
8. Xia W, Zhang J, Kholodenko D, Citron M, Podlisny MB, Teplow DB, Haass C, Seubert P, Koo EH, Selkoe DJ. Enhanced production and oligomerization of the 42-residue amyloid beta-protein by Chinese hamster ovary cells stably expressing mutant presenilins. J. Biol. Chem 1997;272:7977–7982. [PubMed: 9065468]
9. Haass C, Selkoe DJ. Soluble protein oligomers in neurodegeneration: lessons from the Alzheimer's amyloid beta-peptide. Nat. Rev. Mol. Cell. Biol 2007;8:101–112. [PubMed: 17245412]
10. Hardy J, Selkoe DJ. The amyloid hypothesis of Alzheimer's disease: progress and problems on the road to therapeutics. Science 2002;297:353–356. [PubMed: 12130773]
11. Kelleher CT, Chiu R, Shin H, Bosdet IE, Krzywinski MI, Fjell CD, Wilkin J, Yin T, DiFazio SP, Ali J, Asano JK, Chan S, Cloutier A, Girn N, Leach S, Lee D, Mathewson CA, Olson T, O'Connor K, Prabhu AL, Smailus DE, Stott JM, Tsai M, Wye NH, Yang GS, Zhuang J, Holt RA, Putnam NH, Vrebalov J, Giovannoni JJ, Grimwood J, Schmutz J, Rokhsar D, Jones SJ, Marra MA, Tuskan GA, Bohlmann J, Ellis BE, Ritland K, Douglas CJ, Schein JE. A physical map of the highly heterozygous Populus genome: integration with the genome sequence and genetic map and analysis of haplotype variation. Plant J 2007;50:1063–1078. [PubMed: 17488239]
12. LaFerla FM. Calcium dyshomeostasis and intracellular signalling in Alzheimer's disease. Nat. Rev. Neurosci 2002;3:862–872. [PubMed: 12415294]
13. Smith IF, Green KN, LaFerla FM. Calcium dysregulation in Alzheimer's disease: recent advances gained from genetically modified animals. Cell Calcium 2005;38:427–437. [PubMed: 16125228]
14. Huang HM, Ou HC, Hsueh SJ. Amyloid beta peptide enhanced bradykinin-mediated inositol (1,4,5) trisphosphate formation and cytosolic free calcium. Life Sci 1998;63:195–203. [PubMed: 9698049]
15. Mogensen HS, Beatty DM, Morris SJ, Jorgensen OS. Amyloid beta-peptide(25–35) changes [Ca^{2+}] in hippocampal neurons. Neuroreport 1998;9:1553–1558. [PubMed: 9631466]
16. Buxbaum JD, Ruefli AA, Parker CA, Cypess AM, Greengard P. Calcium regulates processing of the Alzheimer amyloid protein precursor in a protein kinase C-independent manner. Proc. Natl. Acad. Sci. U.S.A 1994;91:4489–4493. [PubMed: 8183935]
17. Kuchibhotla KV, Goldman ST, Lattarulo CR, Wu HY, Hyman BT, Bacskai BJ. Abeta plaques lead to aberrant regulation of calcium homeostasis in vivo resulting in structural and functional disruption of neuronal networks. Neuron 2008;59:214–225. [PubMed: 18667150]
18. Herms J, Schneider I, Dewachter I, Caluwaerts N, Kretzschmar H, Van Leuven F, Capacitive calcium entry is directly attenuated by mutant presenilin-1. independent of the expression of the amyloid precursor protein. J. Biol. Chem 2003;278:2484–2489. [PubMed: 12431992]
19. Leissring MA, Akbari Y, Fanger CM, Cahalan MD, Mattson MP, LaFerla FM. Capacitative calcium entry deficits and elevated luminal calcium content in mutant presenilin-1 knockin mice. J. Cell. Biol 2000;149:793–798. [PubMed: 10811821]
20. Yoo AS, Cheng I, Chung S, Grenfell TZ, Lee H, Pack-Chung E, Handler M, Shen J, Xia W, Tesco G, Saunders AJ, Ding K, Frosch MP, Tanzi RE, Kim TW. Presenilin-mediated modulation of capacitative calcium entry. Neuron 2000;27:561–572. [PubMed: 11055438]
21. Leissring MA, Paul BA, Parker I, Cotman CW, LaFerla FM. Alzheimer's presenilin-1 mutation potentiates inositol 1,4,5-trisphosphate-mediated calcium signaling in Xenopus oocytes. J Neurochem 1999;72:1061–1068. [PubMed: 10037477]

22. Smith IF, Hitt B, Green KN, Oddo S, LaFerla FM. Enhanced caffeine-induced Ca^{2+} release in the 3xTg-AD mouse model of Alzheimer's disease. J Neurochem 2005;94:1711–1718. [PubMed: 16156741]
23. Stutzmann GE. Calcium dysregulation IP_3 signaling and Alzheimer's disease. Neuroscientist 2005;11:110–115. [PubMed: 15746379]
24. Stutzmann GE, Caccamo A, LaFerla FM, Parker I. Dysregulated IP_3 signaling in cortical neurons of knock-in mice expressing an Alzheimer's-linked mutation in presenilin1 results in exaggerated Ca^{2+} signals and altered membrane excitability. J Neurosci 2004;24:508–513. [PubMed: 14724250]
25. Green KN, Demuro A, Akbari Y, Hitt BD, Smith IF, Parker I, LaFerla FM. SERCA pump activity is physiologically regulated by presenilin and regulates amyloid beta production. J. Cell. Biol 2008;181:1107–1116. [PubMed: 18591429]
26. Nelson O, Tu H, Lei T, Bentahir M, de Strooper B, Bezprozvanny I. Familial Alzheimer disease-linked mutations specifically disrupt Ca^{2+} leak function of presenilin 1. J. Clin Invest 2007;117:1230–1239. [PubMed: 17431506]
27. Tu H, Nelson O, Bezprozvanny A, Wang Z, Lee SF, Hao YH, Serneels L, De Strooper B, Yu G, Bezprozvanny I. Presenilins form ERCa^{2+} leak channelsa function disrupted by familial Alzheimer's disease-linked mutations. Cell 2006;126:981–993. [PubMed: 16959576]
28. Chakroborty S, Goussakov I, Miller MB, Stutzmann GE. Deviant ryanodine receptor-mediated calcium release resets synaptic homeostasis in presymptomatic 3xTg-AD mice. J Neurosci 2009;29:9458–9470. [PubMed: 19641109]
29. Stutzmann GE, Smith I, Caccamo A, Oddo S, Laferla FM, Parker I. Enhanced ryanodine receptor recruitment contributes to Ca^{2+} disruptions in young, adult, and aged Alzheimer's disease mice. J Neurosci 2006;26:5180–5189. [PubMed: 16687509]
30. Etcheberrigaray R, Hirashima N, Nee L, Prince J, Govoni S, Racchi M, Tanzi RE, Alkon DL. Calcium responses in fibroblasts from asymptomatic members of Alzheimer's disease families. Neurobiol. Dis 1998;5:37–45. [PubMed: 9702786]
31. Hirashima N, Etcheberrigaray R, Bergamaschi S, Racchi M, Battaini F, Binetti G, Govoni S, Alkon DL. Calcium responses in human fibroblasts: a diagnostic molecular profile for Alzheimer's disease. Neurobiol. Aging 1996;17:549–555. [PubMed: 8832629]
32. Ito E, Oka K, Etcheberrigaray R, Nelson TJ, McPhie DL, Tofel-Grehl B, Gibson GE, Alkon DL. Internal Ca^{2+} mobilization is altered in fibroblasts from patients with Alzheimer disease. Proc. Natl. Acad. Sci. U.S.A 1994;91:534–538. [PubMed: 8290560]
33. Leissring MA, LaFerla FM, Callamaras N, Parker I. Subcellular mechanisms of presenilin-mediated enhancement of calcium signaling. Neurobiol. Dis 2001;8:469–478. [PubMed: 11442355]
34. Chan SL, Mayne M, Holden CP, Geiger JD, Mattson MP. Presenilin-1 mutations increase levels of ryanodine receptors and calcium release in PC12 cells and cortical neurons. J. Biol. Chem 2000;275:18195–18200. [PubMed: 10764737]
35. Kasri NN, Kocks SL, Verbert L, Hebert SS, Callewaert G, Parys JB, Missiaen L, De Smedt H. Up-regulation of inositol 1,4,5-trisphosphate receptor type 1 is responsible for a decreased endoplasmic-reticulum Ca^{2+} content in presenilin double knock-out cells. Cell Calcium 2006;40:41–51. [PubMed: 16675011]
36. Stutzmann GE, Smith I, Caccamo A, Oddo S, Parker I, Laferla F. Enhanced ryanodine-mediated calcium release in mutant PS1-expressing Alzheimer's mouse models. Ann. N. Y. Acad. Sci 2007;1097:265–277. [PubMed: 17413028]
37. Cheung KH, Shineman D, Muller M, Cardenas C, Mei L, Yang J, Tomita T, Iwatsubo T, Lee VM, Foskett JK. Mechanism of Ca^{2+} disruption in Alzheimer's disease by presenilin regulation of InsP3 receptor channel gating. Neuron 2008;58:871–883. [PubMed: 18579078]
38. Tandon A, Fraser P. The presenilins. Genome Biol 2002;3:reviews3014. [PubMed: 12429067]
39. Dermaut B, Kumar-Singh S, Engelborghs S, Theuns J, Rademakers R, Saerens J, Pickut BA, Peeters K, van den, Broeck M, Vennekens K, Claes S, Cruts M, Cras P, Martin JJ, Van Broeckhoven C, De Deyn PP. A novel presenilin 1 mutation associated with Pick's disease but not beta-amyloid plaques. Ann. Neurol 2004;55:617–626. [PubMed: 15122701]

40. Raux G, Gantier R, Thomas-Anterion C, Boulliat J, Verpillat P, Hannequin D, Brice A, Frebourg T, Campion D. Dementia with prominent frontotemporal features associated with L113P presenilin 1 mutation. Neurology 2000;55:1577–1578. [PubMed: 11094121]
41. Ionescu L, Cheung KH, Vais H, Mak DO, White C, Foskett JK. Graded recruitment and inactivation of single InsP3 receptor Ca^{2+}-release channels: implications for quantal Ca^{2+} release. J. Physiol 2006;573:645–662. [PubMed: 16644799]
42. Ionescu L, White C, Cheung KH, Shuai J, Parker I, Pearson JE, Foskett JK, Mak DO. Mode switching is the major mechanism of ligand regulation of $InsP_3$ receptor calcium release channels. J. Gen. Physiol 2007;130:631–645. [PubMed: 17998395]
43. Li C, Wang X, Vais H, Thompson CB, Foskett JK, White C. Apoptosis regulation by Bcl-x(L) modulation of mammalian inositol 1,4,5-trisphosphate receptor channel isoform gating. Proc. Natl. Acad. Sci. U.S.A 2007;104:12565–12570. [PubMed: 17636122]
44. Jaimovich E, Mattei C, Liberona JL, Cardenas C, Estrada M, Barbier J, Debitus C, Laurent D, Molgo J, Xestospongin B. a competitive inhibitor of IP_3-mediated Ca^{2+} signalling in cultured rat myotubes isolated myonuclei and neuroblastoma (NG108−15) cells. FEBS Lett 2005;579:2051–2057. [PubMed: 15811317]
45. White C, Li C, Yang J, Petrenko NB, Madesh M, Thompson CB, Foskett JK. The endoplasmic reticulum gateway to apoptosis by Bcl-X(L) modulation of the InsP3R. Nat. Cell. Biol 2005;7:1021–1028. [PubMed: 16179951]
46. Grossmann A, Kukull WA, Jinneman JC, Bird TD, Villacres EC, Larson EB, Rabinovitch PS. Intracellular calcium response is reduced in CD4+ lymphocytes in Alzheimer's disease and in older persons with Down's syndrome. Neurobiol. Aging 1993;14:177–185. [PubMed: 8098135]
47. Oddo S, Caccamo A, Shepherd JD, Murphy MP, Golde TE, Kayed R, Metherate R, Mattson MP, Akbari Y, LaFerla FM. Triple-transgenic model of Alzheimer's disease with plaques and tangles: intracellular Abeta and synaptic dysfunction. Neuron 2003;39:409–421. [PubMed: 12895417]
48. Kang DE, Soriano S, Xia X, Eberhart CG, De Strooper B, Zheng H, Koo EH. Presenilin couples the paired phosphorylation of beta-catenin independent of axin: implications for beta-catenin activation in tumorigenesis. Cell 2002;110:751–762. [PubMed: 12297048]
49. Repetto E, Yoon IS, Zheng H, Kang DE. Presenilin 1 regulates epidermal growth factor receptor turnover and signaling in the endosomal-lysosomal pathway. J Biol Chem 2007;282:31504–31516. [PubMed: 17716970]
50. Foskett JK, White C, Cheung KH, Mak DO. Inositol trisphosphate receptor Ca2+ release channels. Physiol. Rev 2007;87:593–658. [PubMed: 17429043]
51. Green KN, LaFerla FM. Linking calcium to Abeta and Alzheimer's disease. Neuron 2008;59:190–194. [PubMed: 18667147]
52. Hayley M, Perspicace S, Schulthess T, Seelig J. Calcium enhances the proteolytic activity of BACE1: An in vitro biophysical and biochemical characterization of the BACE1-calcium interaction. Biochim. Biophys. Acta 2009;1788:1933–1938. [PubMed: 19486882]
53. Pierrot N, Santos SF, Feyt C, Morel M, Brion JP, Octave JN. Calcium-mediated transient phosphorylation of tau and amyloid precursor protein followed by intraneuronal amyloid-beta accumulation. J. Biol. Chem 2006;281:39907–39914. [PubMed: 17085446]
54. Querfurth HW, Selkoe DJ. Calcium ionophore increases amyloid beta peptide production by cultured cells. Biochemistry 1994;33:4550–4561. [PubMed: 8161510]
55. Mattson MP. Antigenic changes similar to those seen in neurofibrillary tangles are elicited by glutamate and Ca2+ influx in cultured hippocampal neurons. Neuron 1990;4:105–117. [PubMed: 1690014]
56. Mattson MP, Lovell MA, Ehmann WD, Markesbery WR. Comparison of the effects of elevated intracellular aluminum and calcium levels on neuronal survival and tau immunoreactivity. Brain Res 1993;602:21–31. [PubMed: 8448655]
57. Kang DE, Soriano S, Frosch MP, Collins T, Naruse S, Sisodia SS, Leibowitz G, Levine F, Koo EH. Presenilin 1 facilitates the constitutive turnover of beta-catenin: differential activity of Alzheimer's disease-linked PS1 mutants in the beta-catenin-signaling pathway. J. Neurosci 1999;19:4229–4237. [PubMed: 10341227]

58. Kang DE, Yoon IS, Repetto E, Busse T, Yermian N, Ie L, Koo EH. Presenilins mediate phosphatidylinositol 3-kinase/AKT and ERK activation via select signaling receptors. Selectivity of PS2 in platelet-derived growth factor signaling. J. Biol. Chem 2005;280:31537–31547. [PubMed: 16014629]

59. Qin F, Auerbach A, Sachs F. Hidden Markov modeling for single channel kinetics with filtering and correlated noise. Biophys. J 2000;79:1928–1944. [PubMed: 11023898]

60. Qin F, Auerbach A, Sachs F. A direct optimization approach to hidden Markov modeling for single channel kinetics. Biophys. J 2000;79:1915–1927. [PubMed: 11023897]

61. Magleby KL, Pallotta BS. Burst kinetics of single calcium-activated potassium channels in cultured rat muscle. J. Physiol 1983;344:605–623. [PubMed: 6317854]

62. We thank Drs. Rod Eckenhoff and Huafeng Wei for supplying mice, and Dustin Shilling for assistance with the culturing of the PS DKO MEF cells. Acknowledgement is made to the donors of ADR, a program of the American Health Assistance Foundation (A2008-137 to J.K.F.), the Alzheimer's Association (IIRG-08-91662 to D.E.K) and to Core Research for Evolutional Science and Technology of JST, Japan (T.I.). K.-H.C. designed and performed the experiments, analyzed data and wrote the manuscript. L.M. developed recombinant baculoviruses, and performed infections, transfections and cell culture. D.-O.D.M. developed software for modal gating and single cell Ca^{2+} analyses, and assisted in the analyses. I.H. and T.I. developed recombinant baculoviral PS constructs. D.E.K. developed DKO MEF cells. J.K.F. designed and analyzed experiments and wrote the manuscript. None of the authors have competing interests.

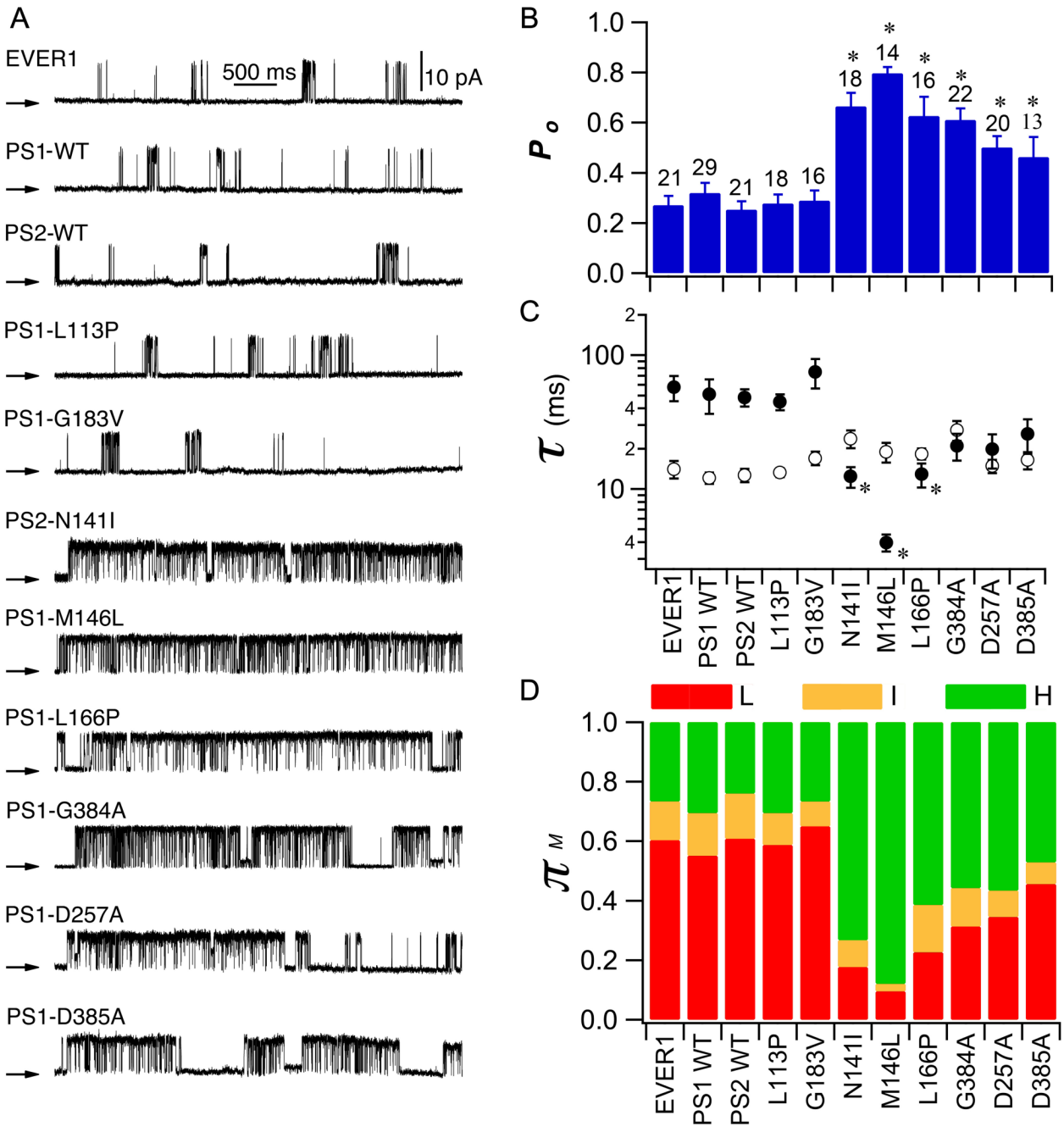

Fig. 1. Effect of recombinant PS on $InsP_3R$ single channel activity in Sf9 cells

(**A**) Representative current recordings (+20 mV) in outer membrane patches of Sf9 cell nuclei infected with different recombinant PS baculoviruses. EVER1 served as an ER membrane protein infection control. Pipette solution contained 1μM free Ca^{2+} and 100 nM $InsP_3$. Arrows indicate closed channel current level in this and all subsequent Figs. Summary of effects of PS on $InsP_3R$ channel P_o (**B**), and mean open time τ_o (open circle) and mean closed time τ_c (filled circle) (**C**). (**D**) Summary of effects of PS on $InsP_3R$ modal gating. Bars: mean ± SEM. Asterisks: $p < 0.05$ by ANOVA compared with EVER1-infected cells.

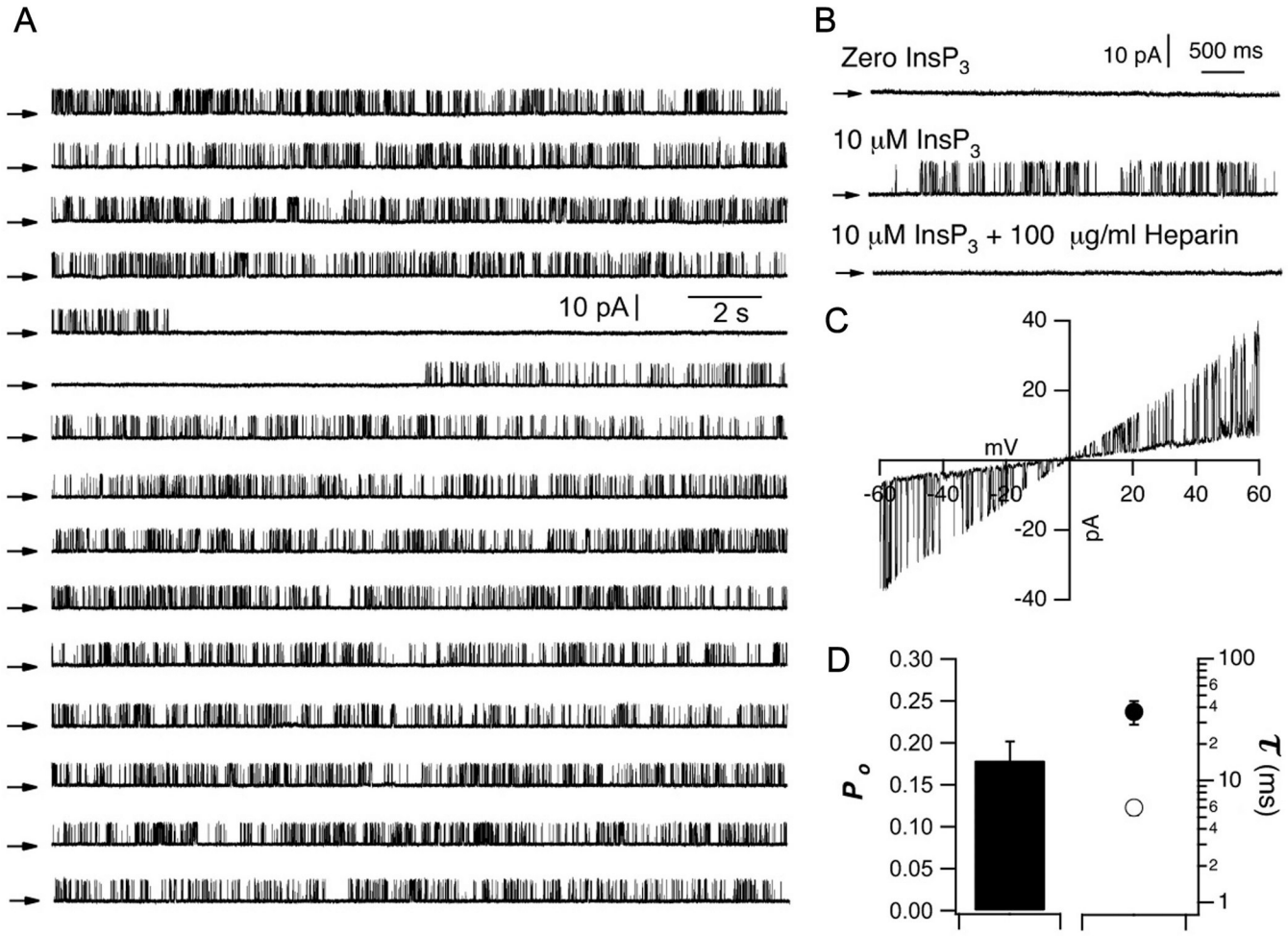

Fig. 2. Characterization of endogenous $InsP_3R$ single channels in human B lymphoblasts

(**A**) Continuous single $InsP_3R$ channel current trace (300 s) recorded from outer membrane of nucleus isolated from human B lymphoblaste at +20 mV with 10 μM $InsP_3$ and 1 μM free Ca^{2+} in pipette solution. Arrows indicate closed channel current levels. (**B**) Representative current traces (+20 mV) in nuclei isolated from human B lymphoblasts. Channel activity required presence of $InsP_3$ (n = 20) and was inhibited by heparin (n = 15). (**C**) *I/V* relationship obtained by ramping holding potential from −60 to +60 mV. (**D**) Summary of $InsP_3R$ channel P_o, and mean open τ_o and closed τ_c durations.

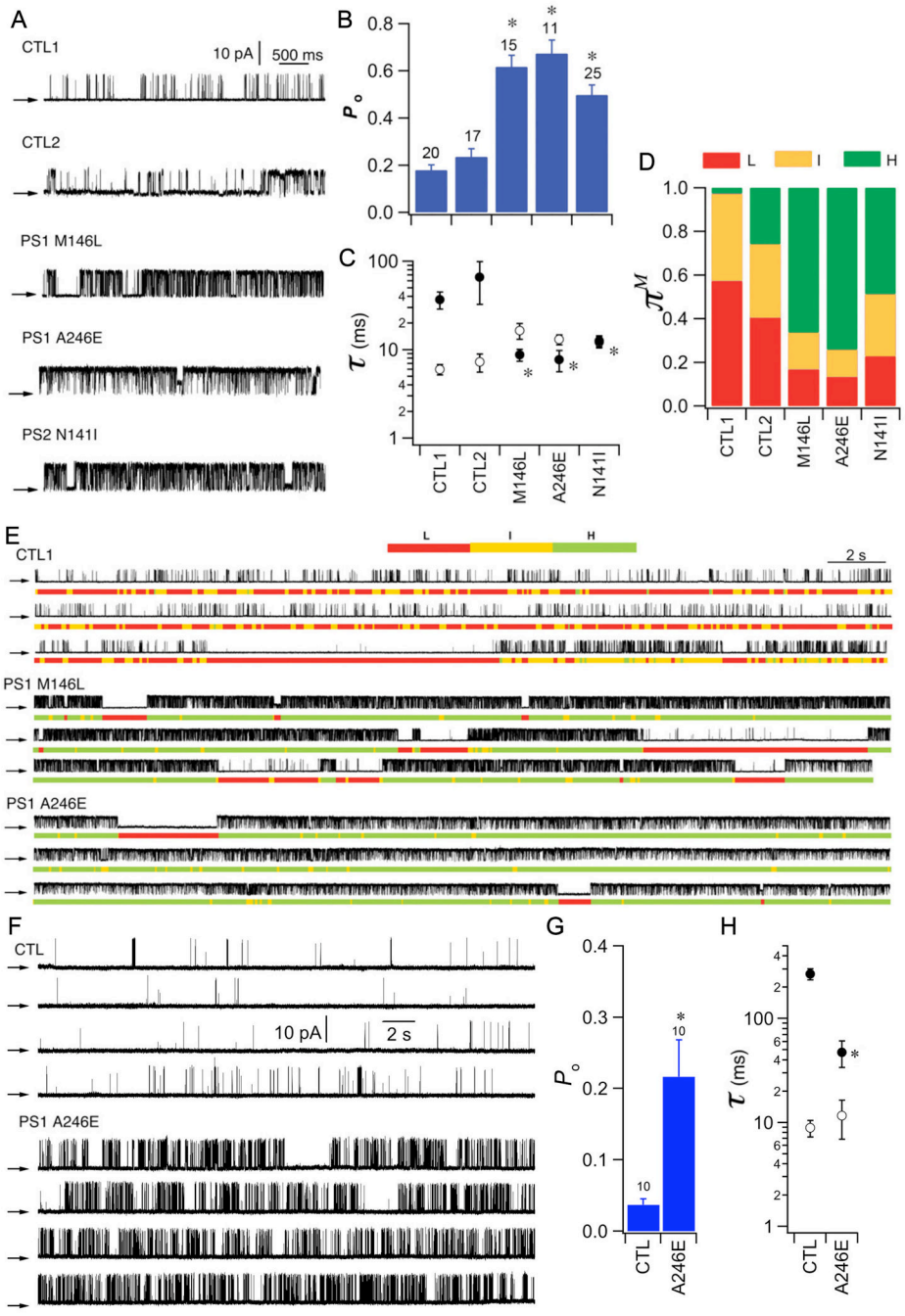

Fig. 3. Effect of FAD PS on $InsP_3R$ gating in human FAD B lymphoblasts

(**A**) Representative $InsP_3R$ currents (+20 mV) in nuclei isolated from human FAD B lymphoblasts and control lymphoblasts from age-matched individuals without FAD activated with 10 μM $InsP_3$ and 1 μM Ca^{2+} in pipette solution. Summary of channel P_o (**B**), τ_o (open circles) and τ_c (filled circles) (**C**) and modal gating analysis (**D**). Asterisks: $p < 0.05$, ANOVA compared with CTL1. (**E**) Modal gating analyses. Each section shows continuous recording with gating mode assignment in color code below. In cells from normal individuals, low P_o is associated with switching between L and I modes. In cells from all three individuals with FAD, enhanced gating is manifested by increased occupancy of H mode at expense of L mode. F-H. Single $InsP_3R$ channel current traces from human B cells activated by sub-optimal $InsP_3$. (**F**)

Representative currents (+20 mV) in isolated nuclei from human FAD lymphoblasts and age-matched control B lymphoblastss activated by sub-optimal 100 nM $InsP_3$ and 1 μM Ca^{2+}. Summary of $InsP_3R$ P_o (**G**), and τ_o (open circle) and τ_c (filled circle) (**H**) from aged-matched control and FAD human B-lymphocblasts. Asterisks: $p < 0.05$ by student's *t*-test.

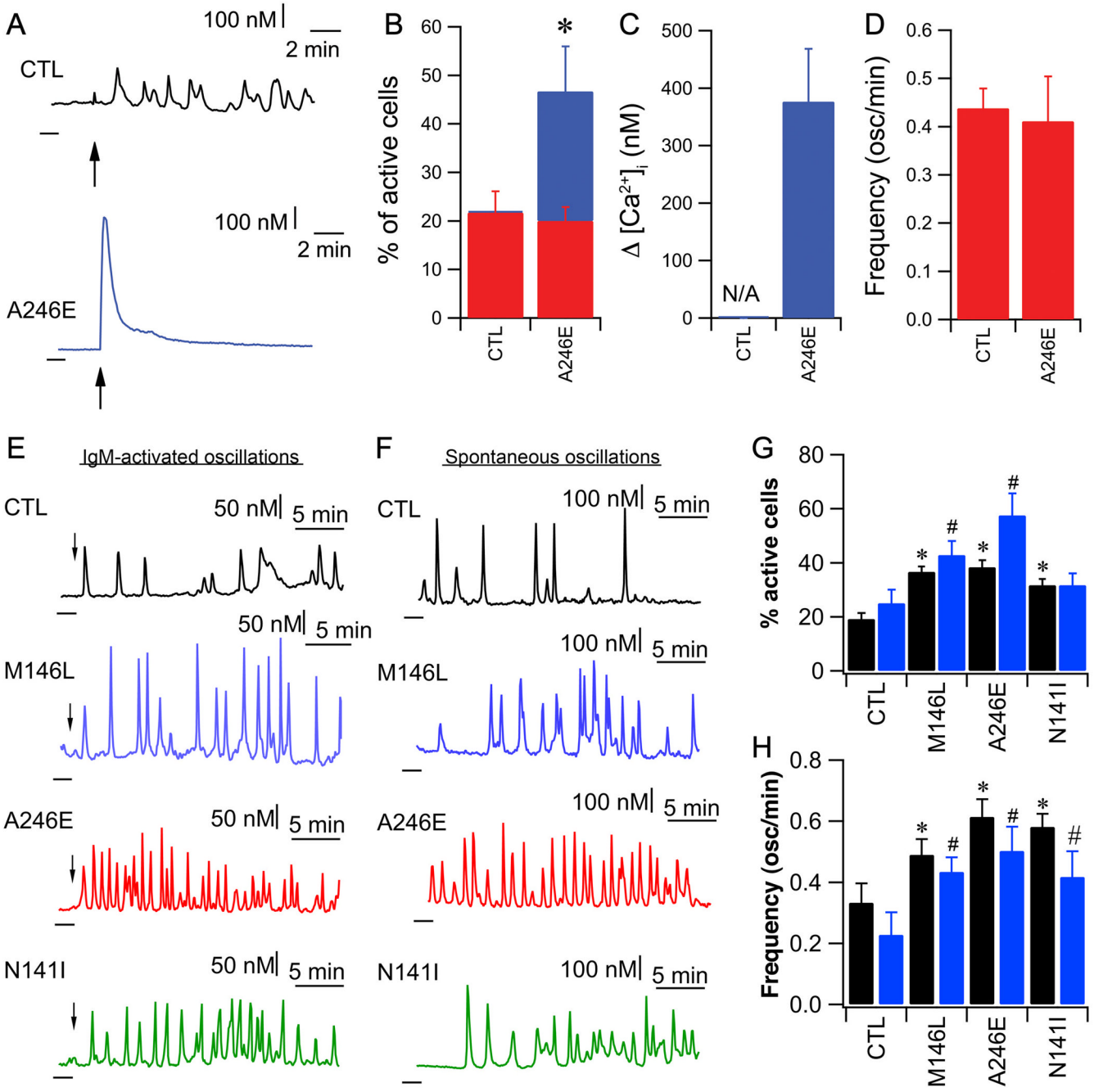

Fig. 4. Exaggerated Ca^{2+} signaling in human FAD B lymphoblasts

(**A**) Representative single cell Ca^{2+} responses to strong IgM stimulation (5μg/ml; arrow) in control human B lymphoblasts (CTL) or FAD lymphoblasts carrying PS1-A246E mutation. Dark lines below and to the left of each trace indicate zero Ca^{2+}. (**B**) Responses to IgM stimulation. Percentages responding with Ca^{2+} oscillations (red) or large amplitude Ca^{2+} transients (blue). (**C**) Summary of peak amplitudes of high-amplitude transient Ca^{2+} responses triggered by 5 μg/ml anti-IgM. (**D**) Ca^{2+} oscillation frequency in response to anti-IgM. N = 3 experiments with 30 cells in each. Asterisk: $p < 0.05$, Student's t-test. (**E**) Representative single cell Ca^{2+} responses to weak IgM stimulation (50 ng/ml; arrow) and (**F**) spontaneous oscillations during perfusion with serum-containing medium in lymphoblasts from unaffected (CTL) and

FAD individuals. Dark lines: zero Ca^{2+} level. (**G**) Percentage of cells responding to IgM (black) or undergoing spontaneous Ca^{2+} oscillations in complete medium (blue). (**H**) Summaries of Ca^{2+} oscillation frequency in response to IgM (black) or spontaneous Ca^{2+} oscillations observed in complete medium (blue). Data in each group summarized from 4 experiments with 30 cells in each. Asterisks or #: $p < 0.05$ by ANOVA as compared with respective controls.

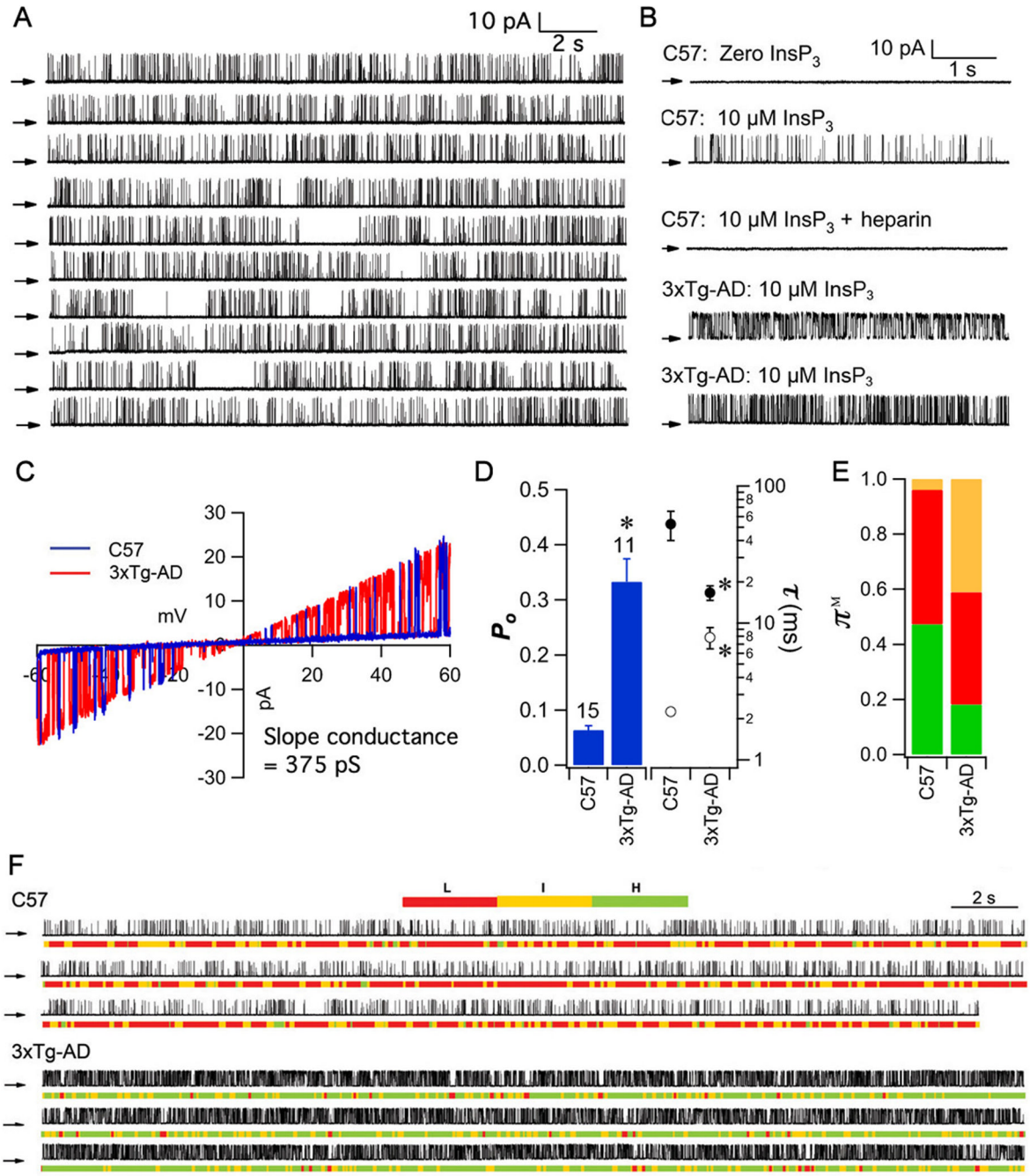

Fig. 5. InsP$_3$R single channel activity in mouse primary embryonic cortical neurons

(**A**) Continuous single InsP$_3$R current trace (200 s) in outer membrane of nucleus isolated from embryonic cortical neuron (+40 mV with 10 μM InsP$_3$ and 1 μM free Ca^{2+} in pipette solution). Arrows: closed channel current level. (**B**) Representative current traces (+40 mV) in nuclei from C57BL/6 (wild type) or 3xTg-AD mice (E14 to E16). Channel activities in both mouse lines required InsP$_3$ and were inhibited by heparin. (**C**) InsP$_3$-activated currents from C57BL/6 (blue) or 3xTg-AD (red) mice were linear with 375 pS slope conductance. (**D**) Summary of InsP$_3$R channel P_o, τ_o and τ_c in cortical neuron nuclei. Bars: mean ± SEM. Asterisks: $p < 0.05$ by unpaired Student's *t*-test. (**E**) Summary of InsP$_3$R modal gating analysis. Colors for gating modes same as Figs 1 and 3. (**F**) Modal gating analysis of InsP$_3$R from cortical neurons. Each

section is a continuous single channel current record with modal assignment indicated by color code. In cells from C57BL/6 mouse, channel gating is alternates between L and I modes, whereas in 3xTg-AD mouse, $InsP_3R$ gating alternates between H and I modes.

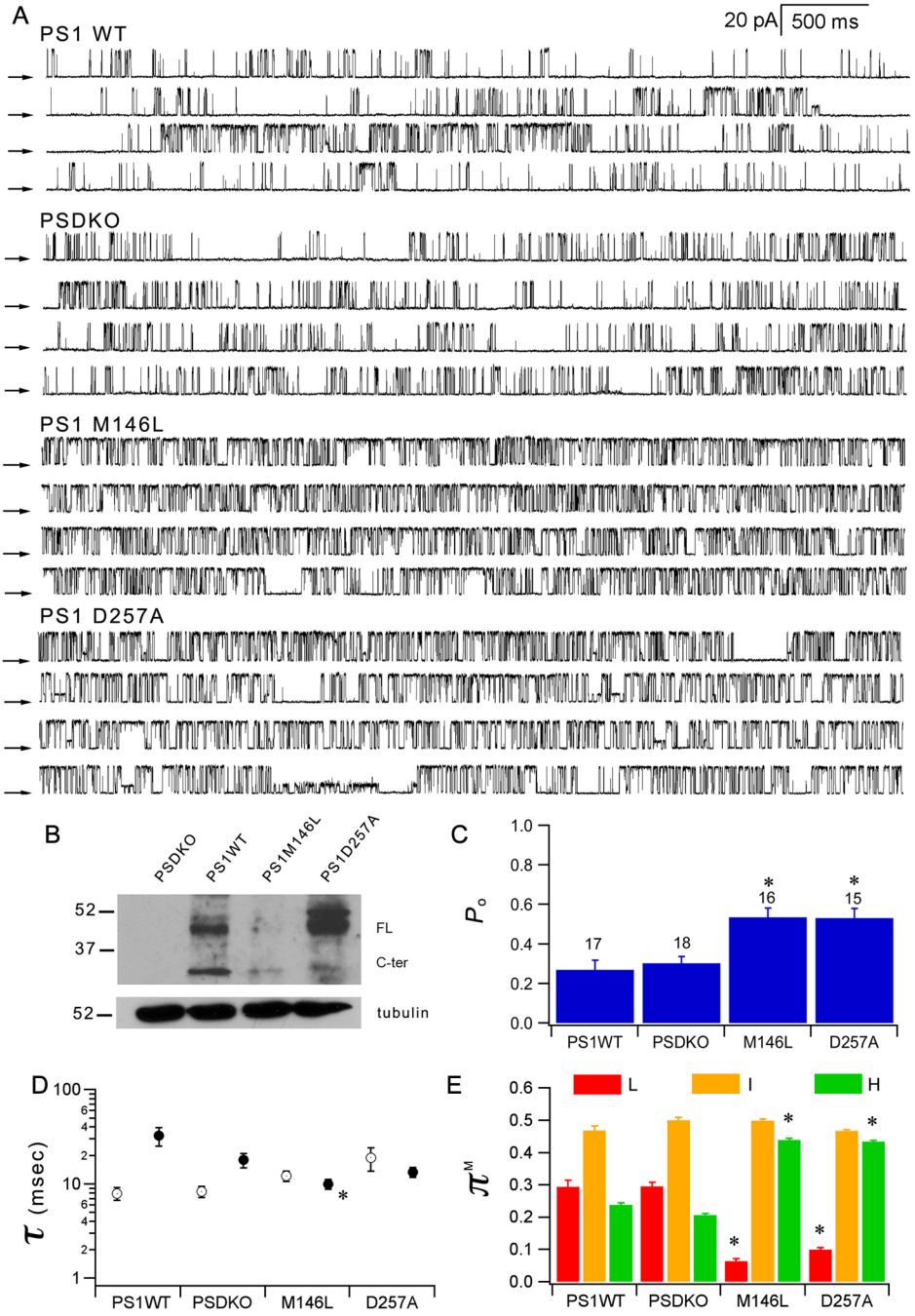

Fig. 6. FAD PS enhances $InsP_3R$ channel gating by gain-of-function effect

(**A**) Continuous single $InsP_3R$ channel current traces recorded from outer membranes of nuclei isolated from PS deficient MEF (PSDKO) and PSDKO stably expressing human PS1-WT, FAD PS1-M146L or secretase-dead PS1-D257A (+40 mV; 10 μM $InsP_3$ and 1 μM free Ca^{2+} in pipette solution). Arrows indicate closed channel current levels. **(B)** Western blot forPS1 in PS-deficient and stably transduced MEF cells. Summary of $InsP_3R$ channel P_o (**C**), τ_o (open circle) and τ_c (filled circle) (**D**) and modal gating analysis (**E**). Asterisks: $p < 0.05$ by ANOVA compared with PSDKO.

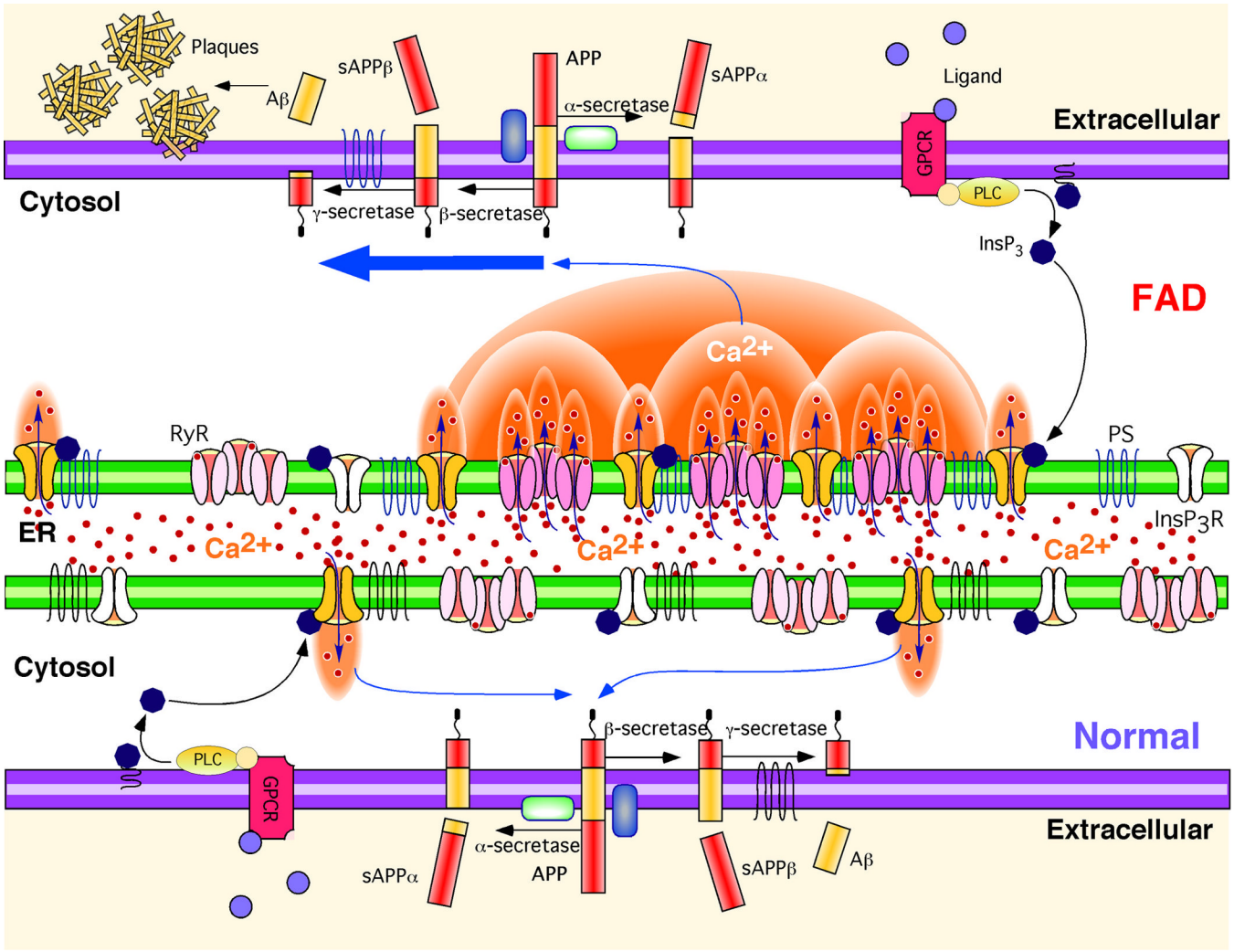

Fig. 7. Hypothetical molecular mechanism of enhanced Aβ production due to Ca^{2+} disruption in FAD PS cells

APP is processed by either α-secretase or β-secretase, the latter leading to Aβ generation after subsequent cleavage by γ-secretase. Stimulation of G-protein coupled receptors (GPCR) or other cell surface receptors by extracellular ligands activates phospholipase C (PLC), which cleaves phosphatidylinositol bisphosphate (PIP_2) to produce $InsP_3$. $InsP_3$ binds to and activates the $InsP_3R$ to release Ca^{2+} from ER stores, increasing cytoplasmic Ca^{2+} concentration. In normal cells, these Ca^{2+} signals are tightly regulated in time, space, and amplitude. In FAD cells, mutant PS exerts stimulatory effects on $InsP_3R$ gating by modal switching to the H mode associated with prolonged channel openings. H mode gating generates exaggerated Ca^{2+} signaling by promoting additional release channel recruitment by CICR. Increased cytosolic Ca^{2+} concentration promotes β-secretase activity (52) and Aβ production (51,54), which, together with mutant PS-enhanced production of amyloidogenic Aβ, results in plaque formation.

Table 1

Human FAD and control B-lymphoblast lines

Cell Line	Genotype	Donor Age/Sex	AD present
AG07877	PS1-M146L	53 / M	Yes
AG06841	PS1-A246E	56 / M	Yes
AG09369	PS2-N141I	56 / M	Yes
AG09180	Normal (CTL1)	56 / M	No
AG08266	Normal (CTL2)	56 / M	No